

A Three-Dimensional Morphometric Analysis of Upper Forelimb Morphology in the Enigmatic Tapir (Perissodactyla: *Tapirus*) Hints at Subtle Variations in Locomotor Ecology

Jamie A. MacLaren^{1*} and Sandra Nauwelaerts^{1,2}

¹Department of Biology, Universiteit Antwerpen, Building D, Campus Drie Eiken, Universiteitsplein, Wilrijk, Antwerp 2610, Belgium

²Centre for Research and Conservation, Koninklijke Maatschappij Voor Dierkunde (KMDA), Koningin Astridplein 26, Antwerp 2018, Belgium

ABSTRACT Forelimb morphology is an indicator for terrestrial locomotor ecology. The limb morphology of the enigmatic tapir (Perissodactyla: *Tapirus*) has often been compared to that of basal perissodactyls, despite the lack of quantitative studies comparing forelimb variation in modern tapirs. Here, we present a quantitative assessment of tapir upper forelimb osteology using three-dimensional geometric morphometrics to test whether the four modern tapir species are monomorphic in their forelimb skeleton. The shape of the upper forelimb bones across four species (*T. indicus*; *T. bairdii*; *T. terrestris*; *T. pinchaque*) was investigated. Bones were laser scanned to capture surface morphology and 3D landmark analysis was used to quantify shape. Discriminant function analyses were performed to reveal features which could be used for interspecific discrimination. Overall our results show that the appendicular skeleton contains notable interspecific differences. We demonstrate that upper forelimb bones can be used to discriminate between species (>91% accuracy), with the scapula proving the most diagnostic bone (100% accuracy). Features that most successfully discriminate between the four species include the placement of the cranial angle of the scapula, depth of the humeral condyle, and the caudal deflection of the olecranon. Previous studies comparing the limbs of *T. indicus* and *T. terrestris* are corroborated by our quantitative findings. Moreover, the mountain tapir *T. pinchaque* consistently exhibited the greatest divergence in morphology from the other three species. Despite previous studies describing tapirs as functionally mediportal in their locomotor style, we find osteological evidence suggesting a spectrum of locomotor adaptations in the tapirs. We conclude that modern tapir forelimbs are neither monomorphic nor are tapirs as conserved in their locomotor habits as previously described. *J. Morphol.* 277:1469–1485, 2016. © 2016 Wiley Periodicals, Inc.

KEY WORDS: discriminant analysis; geometric morphometrics; osteology; scapular fossa ratio; *Tapirus pinchaque*

INTRODUCTION

The Tapiridae (tapirs) represent a deep-rooted clade of large-bodied hoofed mammals within the

order Perissodactyla (odd-toed ungulates). Modern tapirs are widely accepted to belong to a single genus (*Tapirus*), containing four extant species (Hulbert, 1973; Ruiz-García et al., 1985) and several regional subspecies (Padilla and Dowler, 1965; Wilson and Reeder, 2005): the Baird's tapir (*T. bairdii*), lowland tapir (*T. terrestris*), mountain tapir (*T. pinchaque*), and the Malayan tapir (*T. indicus*). Extant tapirs primarily inhabit tropical rainforest, with some populations also occupying wet grassland and chaparral biomes (Padilla and Dowler, 1965; Padilla et al., 1996).

The genus *Tapirus* has frequently been compared morphologically to extinct perissodactyls (Hershkovitz, 2001; Radinsky, 1945; Radinsky, 1986; Rose, 2011; Holbrook, 2013; Colbert, 2013; Holbrook, 1984), earning tapirs the colloquially used title of “living fossil” (Janis, 2011). The title of “living fossil” implies limited changes in tapir skeletal shape throughout evolutionary history (Hershkovitz, 2001; Radinsky, 1945). Evidence supporting the lack of variation in the tapir skeleton through time have focussed on the postcranial elements (Hershkovitz, 2001; Radinsky, 1945), in particular the appendicular skeleton (limbs).

Additional Supporting Information may be found in the online version of this article.

Contract grant sponsors: FWO (Fonds Wetenschappelijk Onderzoek) and BOF-UA (Special Research Fund for Universiteit Antwerpen).

*Correspondence to: Jamie A. MacLaren, Room D 1.41, Building D, Campus Drie Eiken, Universiteitsplein 1, 2610 Antwerp, Belgium. E-mail: jamie.maclaren@uantwerpen.be

Received 22 May 2016; Revised 8 July 2016; Accepted 25 July 2016.

Published online 13 August 2016 in Wiley Online Library (wileyonlinelibrary.com). DOI 10.1002/jmor.20588

Within the Radinsky (1945) study, the upper forelimb description was based on two specimens of *Tapirus pinchaque* (MCZ 6037 and AMNH 149424). He noted several key features common to all tapir forelimbs, including the scapular spine lacking an acromion, an expanded supraglenoid tubercle forming the distal arm of a deep coracoscapular notch, a medially directed anterior hook of greater tubercle of the humerus and the absence of intermediate tubercle or bursa. Assuming the tapir forelimb skeleton has been morphologically conserved through time except in overall size, as suggested by Hershkovitz (2001) and subsequent authors, interspecific differences in limb bone shape would not be expected if analyzed using size-independent shape analyses, such as geometric morphometrics.

Morphometric studies investigating variation in limb morphology have been presented on a range of mammalian species, particularly on carnivores (Van Valkenburgh, 2010; Meloro, 2013; Fabre et al., 2013; Samuels et al., 2007; Martín-Serra et al., 2010; Fabre et al., 2015; Fabre et al., 1982; Fabre et al., 2013) but also rodents (Samuels and Van Valkenburgh, 2007; Kuncova and Frynta, 2011; Elissamburu and de Santis, 2014) and marsupials (Weisbecker and Warton, 2006; Bassarova et al., 2008; Astúa, 2009). Ungulate limb bones have been assessed successfully using geometric morphometrics (e.g., Bernor et al., 2005; Bignon et al., 2005; Curran, 2015, 2013). Geometric morphometrics is a technique for quantifying shape independent of size, often using homologous single points (landmarks) on the surface of a series of objects (Zelditch et al., 2012). This allows quantitative morphometric data to be used for a wide variety of shape analyses. These methods have been used to discriminate populations or species, and detect variation across multiple limb bones of ungulate mammals (Bernor et al., 2005; Bignon et al., 2005; Kaushik, 2013; Martínez-Navarro and Rabinovich, 1994; Curran, 2015; Alrtib et al., 2013).

In this study, we used a three-dimensional geometric morphometric approach to perform a quantitative, comparative study on the upper forelimb skeleton of tapirs. Forelimb morphology has been suggested as a good indicator for terrestrial locomotor ecology (Andersson and Werdelin, 2003; Andersson, 2004; Flores and Díaz, 2012; Halenar, 1992; Hawkins, 1954; Fabre et al., 2013; Fabre et al., 1982), in both extant and extinct taxa. The forelimbs not only provide gravitational support and stability in quadrupedal mammals (Jenkins, 2009; Evans and de Lahunta, 2015) but are also used to an extent in forward propulsion (Watson and Wilson, 2012; Clayton et al., 2012) and shock absorption on ground impact (Payne et al., 2012; Astúa, 2009). Here, we test whether the bones of the tapir upper forelimb exhibit interspecific

variation. Other authors have hypothesized that interspecific differences in the forelimb skeleton of modern tapirs will be minimal (Hershkovitz, 2001; Radinsky, 1945; Padilla and Dowler, 1965). However, the deep temporal divisions between most modern tapir species (Steiner and Ryder, 2001; Ruiz-García et al., 1987; Cozzuol et al., 2012) have offered a broad timescale for adaptive variation based on habitat use and other aspects of tapir ecology. Consequently, we hypothesize that tapir upper forelimbs will exhibit osteological variation that may pertain to differing locomotor ecologies.

MATERIALS AND METHODS

Specimens

A total of 24 fully disarticulated tapir forelimbs (dry bones) were collected from museums in Europe and the United States (Table 1). Multiple specimens of four species of extant tapir (*Tapirus terrestris* [Linnaeus, 1758], *T. pinchaque* [Roulin, 1829], *T. bairdii* [Gill, 1865], and *T. indicus* [Desmarest, 1819]) were collected for analysis to account for intraspecific variation. Morphologically mature limb specimens (adult; Table 1) were used where possible; these were defined based on the full ossification of the scapula cartilage on the dorsal border (Liebich et al., 2011). Specimens with non-ossified dorsal borders (sub-adult; Table 1) were also scanned to maintain high sample sizes; these specimens are noted in Table 1. Sexual dimorphism is present in tapirs (Padilla and Dowler, 1965; de Thoisy et al., 2001), but has been described as non-significant for morphological comparisons (Simpson, 1945) and, therefore, gender bias was not taken into account. To compliment information from published articles on tapir osteology and myology (Murie, 2008; Windle and Parsons, 1902; Campbell, 2007; Bressou, 1936; Pereira, 2013), a dissection was performed on the limbs of a juvenile *Tapirus indicus* that was made available by the Royal Zoological Society of Antwerp (KMDA). Muscular attachments available from the dissection, in addition to published literature, assisted in the description of osteological features and potential functional outcomes. Where necessary, interpretations were supplemented with veterinary accounts of equid osteology and myology (Budras et al., 1999; Liebich et al., 2011; Constantinescu et al., 2014; Clayton et al., 2012).

Scanning

The scapula, humerus, radius, and ulna from one forelimb of each specimen were scanned using a FARO ScanArm Platinum V2 system with integrated FARO Laser Line Probe capable of scanning to a resolution of 50 μm . Bones were suspended using clamps and supports, which were positioned on regions of the specimen surface that landmarks would not be placed on (e.g., shaft of long bone). A three-dimensional virtual point cloud was produced for each limb element, which was visualized in GeoMagic (GeoMagic Qualify v.10, Morrisville, NY). Outlying surfaces in the point clouds were pruned to remove excess surface information (e.g., incidental scanning of clamps or support structures). Point clouds were subsequently converted into detailed polygon-based surface models. Models ranged in detail from 200 k to 1000 k polygons, dependent on the size of the bone and the detail required around joint surfaces.

Geometric Morphometrics

Landmark-based geometric morphometrics is a widely used and appropriate method for quantifying morphological differences between three-dimensional objects (Gould, 2011; Zelditch et al., 2012). The technique is based on landmarks: discrete, biologically (or operationally) homologous points placed onto a series of objects (Zelditch et al., 2012). Type II (maxima and

TABLE 1. List of specimens scanned for geometric morphometric analysis

Taxon	Specimen no.	Skeletal element	Gender	Age class
<i>Tapirus indicus</i>	NMHW 1938	S, H, UR	—	Adult
	NMHW 42298	S, H, UR	Female	Adult
	RMNH 17923	S, H, UR	—	Adult
	RMNH 43543	S, H, R, U	—	Adult
	RMNH 21056	S, H, U	—	Adult
	RMNH 1014	S, H, R, U	—	Adult
	ZMB MAM 47503	S, H, UR	Female	Adult
	ZMB MAM 4950	S, H, UR	—	Adult
	<i>Tapirus bairdii</i>	RMNH 43495	S, H, R, U	—
AMNH 90128		S, H, R, U	—	Sub-adult
AMNH 130104		S, H, R, U	—	Adult
MVZ 141173		S, H, UR	Female	Adult
MVZ 141296		S, H, UR	Male	Sub-adult
<i>Tapirus pinchaque</i>	MNHN 1982-34	S, H, R, U	—	Adult
	MEO 2203a	S, H, UR	Male	Adult
	ZMB MAM 62085	S, H, R, U	Male	Adult
	AMNH 149424	S, H, R, U	Female	Sub-adult
	<i>Tapirus terrestris</i>	NMHW 58178	S, H, UR	Female
MEO 2204e		S, H, R, U	Male	Adult
MEO 2204b		S, H, R, U	Male	Adult
RMNH 12827		S, H, UR	Male	Adult
RMNH 12913		S, H, UR	—	Adult
RMNH 1163.2b		S, H, UR	Male	Adult
ZMB MAM 12999		S, H, UR	Female	Adult

Limb elements used: S = scapula, H = humerus, U = ulna, R = radius, UR = fused ulna and radius (ulnoradius). Dashes represent specimens of unknown gender.

Institutional Abbreviations – **AMNH**, American Museum of Natural History, New York; **MEO**, MuseOs Natuurhistorisch Museum, Koksijde; **MNHN**, Muséum National d'Histoire Naturelle, Paris; **MVZ**, Museum of Vertebrate Zoology, Berkeley; **NMHW**, Naturhistorisch Museum Wien, Vienna; **RMNH**, Naturalis Biodiversity Centre, Leiden; **ZMB**, Museum für Naturkunde, Berlin.

minima) and Type III (calculated from Type II positioning) landmark points were used to define the morphology of the four bones of the shoulder and forearm (stylopodium + zeugopodium). For ease of description, landmarks are labelled with subscript letters pertaining to the bones they describe: for example, scapula (18_SLm), humerus (42_HLms), radius (25_RLms), and ulna (27_ULms; Fig. 1). Finalized surface models were imported into Landmark Editor v.3.0 software (Wiley, 2006) for three-dimensional landmark application. Raw landmark coordinates were exported to MorphoJ v1.06d (Klingenberg, 1992) and aligned using Generalized Procrustes Analysis (GPA). GPA eliminated the effects of size, location and orientation by aligning raw coordinate configurations based on geometric centre (centroid) and minimized distances between corresponding landmarks. The resulting Procrustes coordinates and centroid sizes were then exported from MorphoJ into SPSS v.22 (IBM Corp., 1956) for further analysis. Centroid sizes represent a composite size measure that can be used to scale a configuration of landmarks. The centroid sizes for full adult specimens were retained for intra- and inter-specific size comparisons. A multivariate analysis of variance (MANOVA) was performed on the Procrustes coordinates of the four bones to demonstrate the power of our analysis, given unequal and potentially small sample sizes. The MANOVA was performed in SPSS v.22.

Discriminant Function Analysis

Procrustes coordinates (x, y, z) for all landmarks for each specimen were used in linear discriminant function analysis (DFA), which was used to ascertain what combination of continuous variables could best discriminate between the four groups (species). DFA relies on accurate a priori assignment of specimens to groups, in addition to sample sizes within the groups exceeding the total number of groups under study (Zelditch et al., 2012), although disparate groups can be reliably discriminated with modest to low sample sizes (Lachenbruch, 2014). DFAs were performed in SPSS v.22 (IBM Corp., 1956), entering Procrustes

coordinates using a forward step-wise method to remove independent variables that were not significant to the discrimination process. Predicted group membership, expressed as a % accuracy, was produced and cross-validated by jack-knifing the dataset, producing a classification table. Tests for sensitivity and specificity were also performed and reported in the classification table. The Wilk's lambda test was used to assess whether group means were equal (0 – 1; 0 = highest likelihood of inequality, 1 = high likelihood of group means being equal). Territorial maps were produced to visualize how groups would be classified dependent on the particular discriminant functions. Territorial maps were calculated based on the mean values for each group used in the DFA. These were visualized on linear discriminant function plots, based on the first two discriminant functions (DF1 and DF2). The first two functions account for the highest percentage of variance in the datasets, and were used for graphical representations and discriminant function coefficient interpretation. The third function accounted for between 0.3% and 11.5% of total variance. Cutoff values between groups were determined as the weighted mean of the discriminant scores of the group centroids. Classification tables and territorial maps were created in SPSS v.22 (IBM Corp., 1956), with resultant discriminant function plots formatted in R Studio (R Development Core Team, 2008).

Scapular Fossa Ratio

Initial observations of the tapir scapula suggested interspecific variation in the attachment sites for the large, lateral shoulder muscles: the scapular fossae. The scapular fossae (supraspinous and infraspinous) represent principle origination sites for the supraspinatus and infraspinatus muscles, which together act to support, extend (both *m. supraspinatus*), and flex (*m. infraspinatus*) the shoulder. To compliment the interpretation of discriminant function results of the scapula, scapular fossa ratios (SFR) were calculated from adult specimens of all taxa (Table 1). Areas of the two lateral scapular fossae were calculated by pruning the 3D-laser scans in GeoMagic

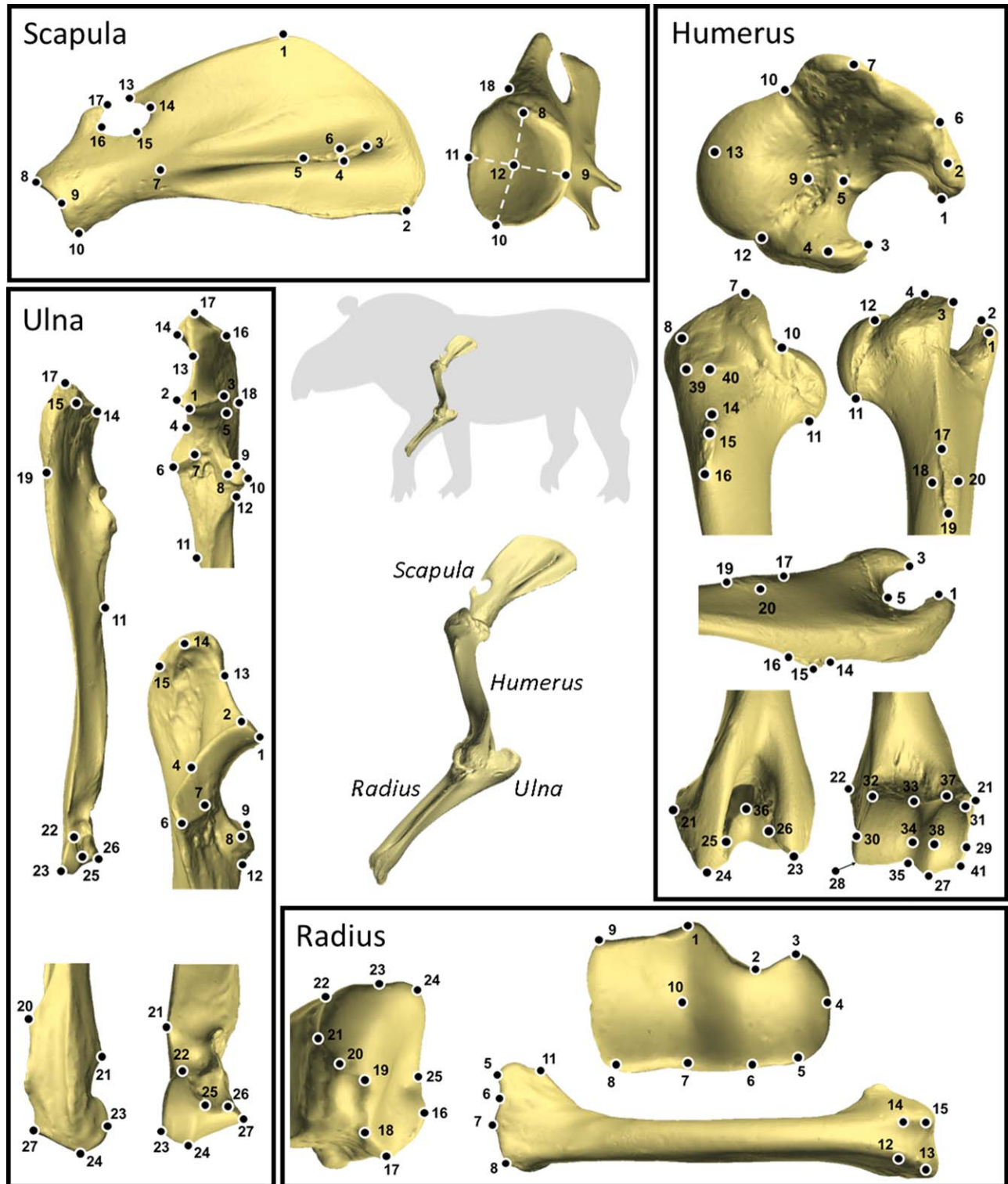


Fig. 1. Three-dimensional landmark placements on four largest forelimb bones of *Tapirus*. Placement of bones within forelimb tapir (centre). Landmark placement exemplified on bones of *Tapirus pinchaque* (MEO 2203a). Descriptions of landmark placements can be found in the Supporting Information.

TABLE 2. Jack-knifed classification table of specimen assignments for scapula, humerus, radius, and ulna using linear discriminant analysis

	Species	Predicted species membership				Total	Sensitivity	Specificity
		<i>T. bai</i>	<i>T. ind</i>	<i>T. pin</i>	<i>T. ter</i>			
Scapula								
Specimen	<i>T. bairdii</i>	5	0	0	0	5	1.000	1.000
Count	<i>T. indicus</i>	0	8	0	0	8	1.000	1.000
	<i>T. pinchaque</i>	0	0	4	0	4	1.000	1.000
	<i>T. terrestris</i>	0	0	0	7	7	1.000	1.000
Overall % correctly classified:						100		
Humerus								
		<i>T. bai</i>	<i>T. ind</i>	<i>T. pin</i>	<i>T. ter</i>			
Specimen	<i>T. bairdii</i>	5	0	0	0	5	1.000	1.000
Count	<i>T. indicus</i>	0	8	0	0	8	1.000	1.000
	<i>T. pinchaque</i>	0	0	4	0	4	1.000	1.000
	<i>T. terrestris</i>	2	0	0	5	7	1.000	0.714
Overall % correctly classified:						91.7		
Radius								
		<i>T. bai</i>	<i>T. ind</i>	<i>T. pin</i>	<i>T. ter</i>			
Specimen	<i>T. bairdii</i>	5	0	0	0	5	1.000	1.000
Count	<i>T. indicus</i>	0	7	0	0	7	1.000	1.000
	<i>T. pinchaque</i>	0	0	4	0	4	1.000	1.000
	<i>T. terrestris</i>	1	0	0	6	7	1.000	0.857
Overall % correctly classified:						95.7		
Ulna								
		<i>T. bai</i>	<i>T. ind</i>	<i>T. pin</i>	<i>T. ter</i>			
Specimen	<i>T. bairdii</i>	5	0	0	0	5	1.000	1.000
Count	<i>T. indicus</i>	0	8	0	0	8	1.000	1.000
	<i>T. pinchaque</i>	0	0	4	0	4	1.000	1.000
	<i>T. terrestris</i>	2	0	0	5	7	1.000	0.714
Overall % correctly classified:						91.7		

(GeoMagic Qualify v.10). These were imported into MeshLab (Cignoni et al., 2013) to calculate surface area (A). SFRs were calculated using the equation:

$$\frac{A_{\text{supraspinous}}}{A_{\text{supraspinous}} + A_{\text{infraspinous}}}$$

For comparison with other perissodactyl scapulae, three specimens of equids (*Equus przewalski* MEO 2194f; *E. hemionus* NMW 7795; and *E. quagga* RMCA 4094) and two specimens of rhinoceros (*Ceratotherium simum* RMCA 35146; and *Diceros bicornis* RMCA 31727) were added to the analysis of SFR. Differences between groups were assessed using one-way analysis of variance (ANOVA) and Tukey HSD (honest significant difference) post hoc test for significant differences, both performed in SPSS v.22 (IBM Corp., 1956).

RESULTS

Overall, linear discriminant functions that successfully discriminated between the four species of extant tapirs were calculated for the scapula, humerus, ulna, and radius. A classification table with both original and jack-knifed classifications (reporting sensitivity and specificity results) is used to quantify the success of discrimination between species for each bone (Table 2). Accuracy of jack-knifed species classification exceeds 90% for all upper forelimb bones, with the scapula representing the most diagnostic bone with 100% accurate discrimination between the four species. The radius is the second most diagnostic bone with a classification accuracy of 95.7%. *Tapirus indicus* and *T. pinchaque* are consistently discriminated across all bones with 100% accuracy. However, at least one specimen of *T.*

terrestris was misclassified for three bones (humerus, radius, and ulna). Wilks' lambda testing revealed that for all bones the group centroids were significantly different ($\lambda < 0.001$). Function scores at group centroids (canonical group means; mean group position in canonical variate-space) are reported in Table 3, with cut-off scores based on weighted mean discriminant scores between two group centroids reported in Table 4. Linear discriminant plots for each bone are presented in Figure 2, with discriminant function coefficients (loadings) for landmarks that contribute toward accurate discrimination highlighted in Table 5. Results of the power analyses revealed statistical power for the scapula, humerus, and ulna in excess of 0.8 (high power); the radius recorded a power of 0.52 (medium power).

Scapula

Linear discriminant function plots of the scapula reveal isolated occupation of variate-space by each tapir species. The first two linear discriminant functions (DF1 & 2) based on the scapula landmarks account for 88.5% of variance (Fig. 2a). Scapulae from each species were classified correctly 100% both prior to and after jack-knifing (Table 2). The analysis was revealed as both highly sensitive (1.000) and specific (1.000), with no false positive or negative results. Discriminant functions at the group centroids show that taxa overlapping along one DF show separation along the other DF (Fig. 2; Tables 3 and 4); both DFs are necessary for successful discrimination between species. The proximodistal

TABLE 3. Discriminant functions at group centroids

Scapula	Discriminant function		Humerus	Discriminant function	
Species	1	2	Species	1	2
<i>T. bairdii</i>	-5.154	3.163	<i>T. bairdii</i>	-17.145	-3.477
<i>T. indicus</i>	0.013	1.881	<i>T. indicus</i>	4.434	10.13
<i>T. pinchaque</i>	-6.837	-5.466	<i>T. pinchaque</i>	39.467	-7.458
<i>T. terrestris</i>	7.573	-1.286	<i>T. terrestris</i>	-15.374	-4.832
Radius	Discriminant function		Ulna	Discriminant function	
Species	1	2	Species	1	2
<i>T. bairdii</i>	3.869	2.73	<i>T. bairdii</i>	3.06	-1.005
<i>T. indicus</i>	4.063	-4.872	<i>T. indicus</i>	-6.696	-0.829
<i>T. pinchaque</i>	-23.318	0.396	<i>T. pinchaque</i>	1.716	7.345
<i>T. terrestris</i>	6.498	2.696	<i>T. terrestris</i>	4.486	-2.531

positioning of the cranial angle (ς Lm 1) and the mediolateral placement of the *m. biceps brachii* origin (ς Lm 18) influence both DF1 and DF2; the lateral expansion of the glenoid cavity (ς Lm 9) also influences discrimination along DF1. Landmarks that show greatest discrimination along DF2 include the craniocaudal enlargement of the scapular spine tuberosity (ς Lm 3), the proximodistal expansion of the cranial margin of the glenoid cavity (ς Lm 8), and the proximal-most point of the supraglenoid tubercle (ς Lm 17) (Fig. 2; Table 5). Centroid size varies both inter- and intra-specifically, with *T. terrestris* and *T. bairdii* exhibiting the greatest range of centroid sizes. *T. indicus* show the largest mean average centroid size (409.79 ± 16). *T. terrestris* display the largest individual centroid size (431.45). *T. bairdii* displays a smaller mean centroid size (379.76 ± 30) to that of *T. terrestris* (399.17 ± 25), with *T. pinchaque* displaying the smallest (352.69 ± 13).

SFRs for the four tapir species and two perisso-dactyl outgroups are presented in Figure 3.

Results from Tukey HSD post hoc testing from ANOVA of SFRs revealed that *T. indicus* was significantly separate from all Neotropical taxa ($P < 0.01$; Table 6). *T. bairdii* does not differ significantly from other Neotropical species, whereas *T. pinchaque* is statistically separated from *T. terrestris* ($P = 0.048$). The exclusion of a single outlying *T. terrestris* (MEO 2204e) polarises this result with a very strong significant difference ($P < 0.01$). The highest SFR is calculated for *T. pinchaque*, with a mean SFR of 0.610 ± 0.03 . Mean SFRs in the larger Neotropical species were similar to one another: *T. terrestris* (0.557 ± 0.03) and *T. bairdii* (0.572 ± 0.01). *T. indicus* displayed a mean SFR closer to extant rhinoceroses than to other extant tapirs (Fig. 3). *Equus* displayed the lowest SFR of the species studied (mean SFR: 0.363 ± 0.01).

Humerus

Linear discriminant function plots of the humerus show a substantial separation between three

TABLE 4. Discrimination between species based on cut-off scores on either Discriminant Function 1 or Discriminant Function 2

	Description of discrimination
Scapula	
Discriminant function 1	<i>T. bairdii</i> + <i>T. pinchaque</i> < -0.989 < <i>T. indicus</i> < 2.023 < <i>T. terrestris</i> (discriminates between 3 of 4 groups; <i>T. bairdii</i> and <i>T. pinchaque</i> not separated)
Discriminant function 2	<i>T. pinchaque</i> < -0.815 < <i>T. bairdii</i> (discriminates between <i>T. bairdii</i> and <i>T. pinchaque</i>)
Humerus	Description of discrimination
Discriminant function 1	<i>T. bairdii</i> + <i>T. terrestris</i> < -2.444 < <i>T. indicus</i> < 13.895 < <i>T. pinchaque</i> (discriminates between 3 of 4 groups; <i>T. bairdii</i> and <i>T. terrestris</i> not separated)
Discriminant function 2	1.075 < <i>T. indicus</i> (discriminates <i>T. indicus</i>)
Radius	Description of discrimination
Discriminant function 1	<i>T. pinchaque</i> < -5.403 (discriminates <i>T. pinchaque</i>)
Discriminant function 2	<i>T. indicus</i> < -0.759 (discriminates <i>T. indicus</i> ; <i>T. bairdii</i> and <i>T. terrestris</i> not separated)
Ulna	Description of discrimination
Discriminant function 1	<i>T. indicus</i> < -0.699 (discriminates <i>T. indicus</i> ; <i>T. bairdii</i> and <i>T. terrestris</i> not separated)
Discriminant function 2	<i>T. pinchaque</i> < 2.310 (discriminates <i>T. pinchaque</i>)

Cut-off scores (means) weighted by number of specimens per group.

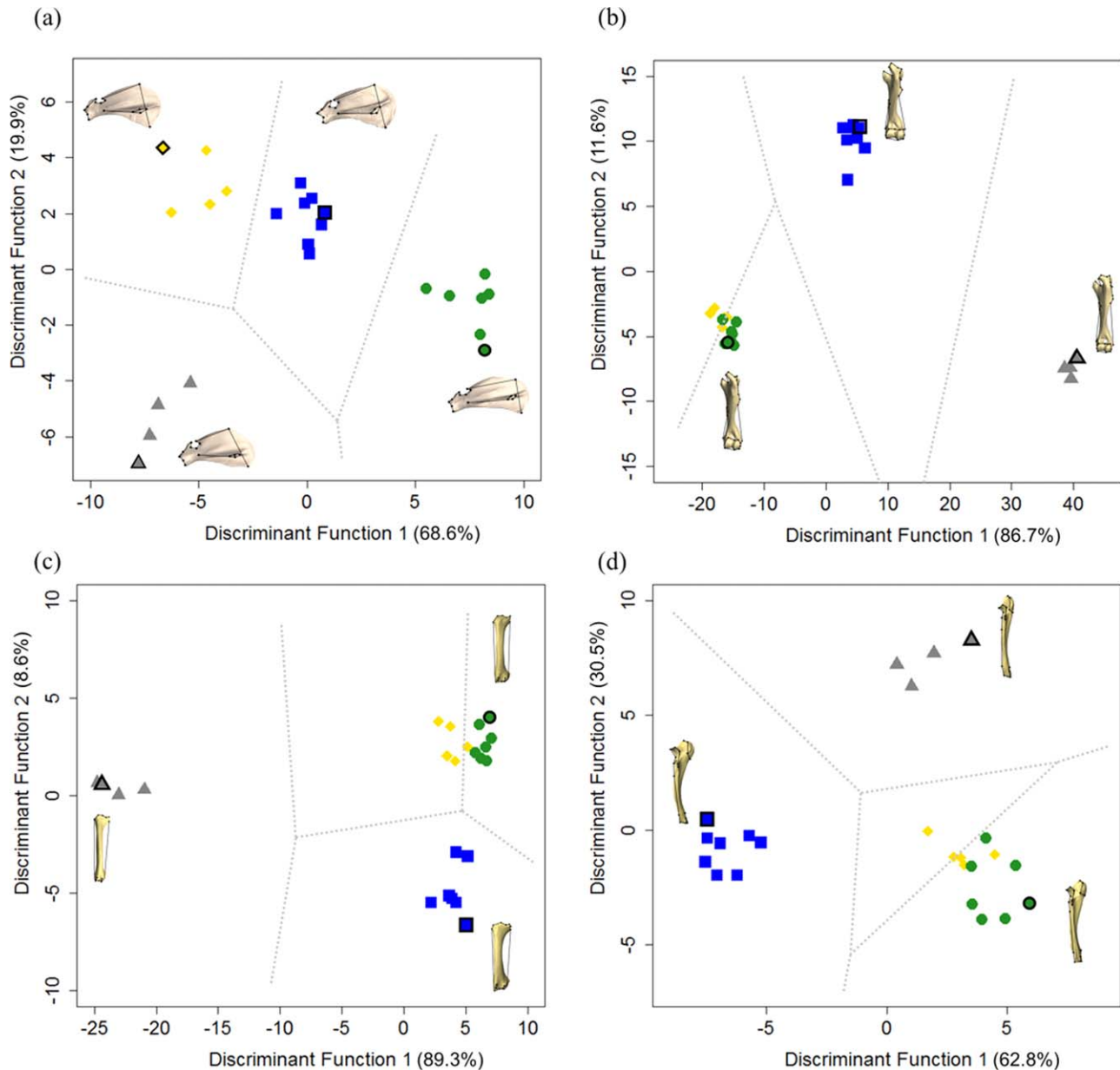


Fig. 2. Linear discriminant function plots for the upper forelimb bones of four extant species of *Tapirus*. Discriminant function plots of (a) scapula, (b) humerus, (c) radius, and (d) ulna of extant *Tapirus* species. Percentage of variance accounted for by each discriminant function is presented in brackets. Species key: *T. bairdii* = gold diamonds; *T. indicus* = blue squares; *T. pinchaque* = gray triangles; *T. terrestris* = green circles; dotted line = territorial map lines separating each group based on mean average values. Outlined points and representative bone morphologies denote specimens furthest from other species clusters.

groups: *T. indicus*, *T. pinchaque* and a combined *T. bairdii* + *T. terrestris* grouping (Fig. 2b). Combined, DF1 and DF2 account for 98.3% of humeral variance; DF1 alone accounting for 86.7% of humeral variance (Fig. 2b). Humeri from all species are classified 100% correctly; in addition *T. indicus*, *T. bairdii*, and *T. pinchaque* are correctly classified 100% when classifications are jack-knifed. 28.6% of *T. terrestris* (two specimens: RMNH 12913 and ZMB MAM 12999) are incorrectly classified as *T. bairdii*. Overall, tapir humeri

are correctly classified 91.7% after jack-knifing (Table 2). This humeral discriminant analysis was shown to be highly sensitive (1.000); two false positives were reported, and thus specificity fell to 0.714 (Table 2). Functions at the group centroids support the presence of three morphotypes, with *T. terrestris* and *T. bairdii* group centroids falling very close to one another, but far separated from *T. indicus* and *T. pinchaque* along both DF1 and DF2 (Fig. 2; Tables 3 and 4). DF1 successfully discriminates between the three morphotypes

TABLE 5. Standardized linear discriminant function coefficients for upper arm bones of *Tapirus*

Scapula* boneLm n_{axis}	Discriminant functions		Humerus† boneLm n_{axis}	Discriminant functions	
	1	2		1	2
$sLm 1_x$	1.855	-1.346	$Hm 2_y$	1.255	-0.768
$sLm 3_y$	-0.255	1.597	$Hm 2_z$	-0.471	-1.173
$sLm 5_x$	-0.017	-0.782	$Hm 4_x$	2.052	-1.024
$sLm 6_y$	0.814	0.715	$Hm 7_x$	1.439	1.687
$sLm 8_z$	-0.716	-1.454	$Hm 11_y$	-2.509	0.231
$sLm 9_x$	2.004	-0.159	$Hm 18_x$	5.11	-0.507
$sLm 17_y$	-0.484	1.284	$Hm 22_z$	5.69	1.00
$sLm 18_z$	-1.31	1.017	$Hm 26_x$	-6.333	0.319
			$Hm 27_x$	-5.77	-1.297
			$Hm 29_y$	1.953	0.622
			$Hm 30_z$	8.881	1.269
			$Hm 41_y$	2.802	0.375

Radius‡ boneLm n_{axis}	Discriminant functions		Ulna§ boneLm n_{axis}	Discriminant functions	
	1	2		1	2
$Rm 1_x$	2.764	-0.436	$Um 2_x$	-0.985	1.163
$Rm 4_x$	4.247	1.594	$Um 11_x$	1.321	0.709
$Rm 4_y$	5.036	0.851	$Um 15_x$	0.558	1.791
$Rm 9_z$	-5.347	-0.706	$Um 16_y$	0.43	0.214
$Rm 10_x$	2.003	0.91	$Um 18_z$	0.813	-0.171
$Rm 10_z$	-2.478	-1.753	$Um 19_x$	0.446	1.643
$Rm 11_y$	-5.4	-0.29	$Um 20_z$	-1.336	0.912
$Rm 14_x$	8.086	1.276	$Um 24_z$	-1.23	0.293
$Rm 20_x$	2.954	0.714			

Bold numbers highlight coordinates of greatest influence for each discriminant function.

*Threshold for interpretation of Function: 1 = >1; 2 = >1.

†Threshold for interpretation of Function: 1 = >5; 2 = >1.

‡Threshold for interpretation of Function: 1 = >5; 2 = >1.

§Threshold for interpretation of Function: 1 = >1; 2 = >1.

present. Morphological features that contribute most toward accurate interspecific classifications along DF1 include the proximodistal positioning of the distal margin of the teres major tuberosity ($Hm 18$) and the craniocaudal expansion of the medial humeral condyle ($Hm 22, 26, 27, 30$). Classification along DF2 (accounting for 11.6% of variance) is influenced by the medial deflection of the greater tubercle ($Hm 2$) and the proximal expansion of the lesser tubercle ($Hm 4, 9$); in addition DF2 is also influenced by the mediolateral and craniocaudal expansion of the humeral condyle ($Hm 22, 26, 27, 30$) (Figs. 1 and 2; Table 5). Humeral centroid size is greatest in the largest species, *T. indicus* (individual: 724.55; mean average: 689.92 ± 21). The smallest species by body mass (*T. pinchaque*) displays the second largest average humeral centroid size (681.67 ± 12), with *T. terrestris* exhibiting the smallest (642.09 ± 34).

Radius

Linear discriminant function plots of the radius show a large separation of *T. pinchaque* from the other taxa, with *T. terrestris* and *T. bairdii* again showing some spatial overlap (Fig. 2c). The first discriminant function (DF1) accounts for 89.3% of radial variance, with DF2 accounting for only 8.6%. Radii from all species are classified 100%

correctly prior to jack-knifing. One specimen of *T. terrestris* (MEO 2204e) was incorrectly classified as *T. bairdii* after jack-knifing, resulting in an overall classification accuracy of 95.7%. Radial discriminant analysis was highly sensitive (1.000); a single false positive was reported, reducing specificity 0.857. Functions at the group centroids show that *T. pinchaque* is far removed from the other taxa along DF1, with the other three species possessing similar mean discriminant functions along DF1 (Fig. 2; Tables 3 and 4). *T. bairdii* and *T. terrestris* group centroids are very similarly placed on DF2 (*T. bairdii* = 2.730; *T. terrestris* = 2.696). This similar placement for three species may account for only medium power for the radius compared to high power for all other bones. Both *T. indicus* and *T. pinchaque* group centroids are positioned separate to the *T. bairdii* + *T. terrestris* group along DF2 (Fig. 2; Tables 3 and 4). Positioning along DF1 is influenced by the lateral deflection ($Rm 4, 11$) and craniocaudal expansion ($Rm 9$) of the fovea of the radial head, in addition to the proximodistal positioning of $Rm 14$ (apex of lateral border of the *m. extensor carpi radialis* groove). $Rm 14$ also contributes to discrimination along DF2, in addition to both the lateral expansion ($Rm 4$) and the positioning of the deepest point on the medial sagittal crest of the fovea

capitis radii (r_{Lm} 10). Average centroid size of the radius is notably larger in *T. indicus* (575.91 ± 15). The radii of both *T. bairdii* and *T. pinchaque* show similar average centroid sizes (527.53 ± 27 and 521.01 ± 19 respectively). As in the humerus, *T. terrestris* exhibits the smallest average radial centroid size (506.63 ± 26).

Ulna

Linear discriminant function plots of the ulna show a large separation of *T. pinchaque* from the other American taxa, with *T. terrestris* and *T. bairdii* again showing some spatial overlap. As in all other plots, *T. indicus* positions away from the American species (Fig. 2d). The first two discriminant functions account for 93.3% of ulna variance (DF1 = 62.8%; DF2 = 30.5). Ulnae from all species are classified 100% correctly. Jack-knifed ulna classification falls to 91.7% accuracy, with two *T. terrestris* specimens (RMNH 12827 and RMNH 1163.2b) incorrectly classified as *T. bairdii* (Table 2). Ulnar discriminant analysis was shown to be highly sensitive (1.000). Two false positives were reported, reducing specificity to 0.714 (Table 2). Ulnar functions at group centroids show that *T. indicus* is far removed from the other taxa along DF1, with centroid and cut-off points all present in negative DF1 variate-space (Fig. 2; Tables 3 and 4). *Tapirus bairdii* and *T. terrestris* group centroids are positioned close to each other for both DF1 and DF2, representing a *T. bairdii* + *T.*

TABLE 6. Tukey HSD (honest significance difference) test for significant differences between scapular fossa ratios in *Tapirus*

	<i>T. bairdii</i>	<i>T. indicus</i>	<i>T. pinchaque</i>	<i>T. terrestris</i>
<i>T. bairdii</i>		<0.001	0.122	0.338
<i>T. indicus</i>	<0.001		<0.001	<0.001
<i>T. pinchaque</i>	0.122	<0.001		0.048
<i>T. terrestris</i>	0.338	<0.001	0.048	

Significant differences set at $P \leq 0.05$, with significant values in bold.

terrestris ulnar morphotype. Both the group centroid and cut-off points for *T. pinchaque* are found in positive DF2 variate-space (Fig. 2; Tables 3 and 4), whereas group centroids for all other species are placed in negative DF2 variate-space. Discrimination along DF1 is influenced by the proximodistal positioning of the lateral coronoid process ($\cup Lm$ 11), the craniocaudal depth of the distal ulna ($\cup Lm$ 20) and the mediolateral narrowing of the pisiform facet ($\cup Lm$ 24; Fig. 1; Table 5). Discrimination on DF2 is influenced by the morphology of the medial anconeal process ($\cup Lm$ 2), the proximodistal positioning of the *m. triceps brachii* insertion (on the olecranon tuber; $\cup Lm$ 15), and the lower margin of the *m. palmaris longus* origination ($\cup Lm$ 19; Fig. 1; Table 5). Average ulnar centroid size is largest in *T. indicus* (572.75 ± 14). Similarly to the radius and humerus, *T. bairdii* and *T. pinchaque* display comparable average centroid sizes (527.70 ± 25 and 525.44 ± 21 , respectively) for the ulna. *T. terrestris* exhibits the smallest average ulnar centroid size (501.77 ± 24).

DISCUSSION

The results support our hypothesis of interspecific variation in modern tapir upper forelimbs. Linear discriminant function analyses revealed interspecific patterns across all upper limb bones. The scapula is the only bone to be 100% successfully discriminated across all species. Our MANOVA results suggest that sample sizes in this study are more than sufficient to test interspecific differences (statistical power between 0.52 and 0.87), despite superficially low specimen counts. Results may suffer from assumptions associated with discriminant analyses (Zelditch et al., 2012). For example, the number of specimens of *T. pinchaque* does not exceed the number of predetermined groups ($n = 4$). In addition, there may be an over-reliance on accurate species identification *a priori*, especially as we did not conduct a corresponding genetic analysis on the specimens under study. Nevertheless, we are confident in the power of our analysis, and here present the major morphological variations within our sample of extant tapirs, with functional interpretations. The divergent upper forelimb morphology of the mountain

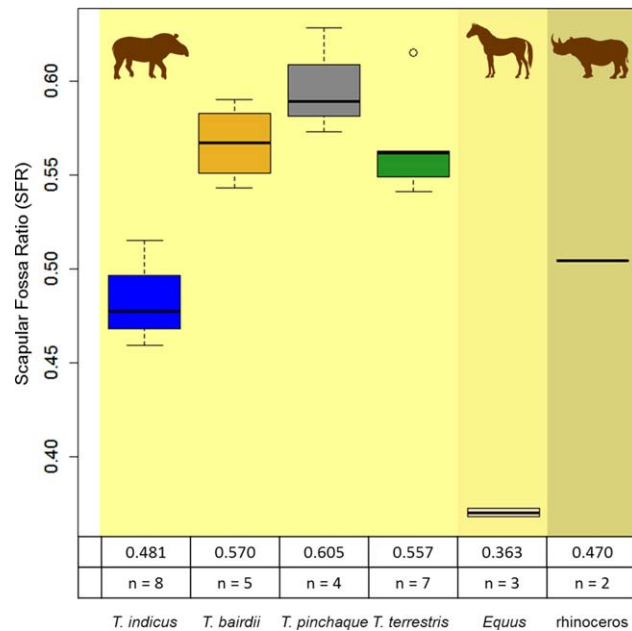


Fig. 3. Scapular fossa ratios (SFRs) for four extant tapir species and representatives of other modern perissodactyls (equids and rhinocerotids). Mean SFR and number of specimens (n) included below box-plot. Black line = median value. Black circles = statistical outlier. Silhouettes represent the relevant families of perissodactyl (from left: Tapiridae, Equidae, Rhinocerotidae).

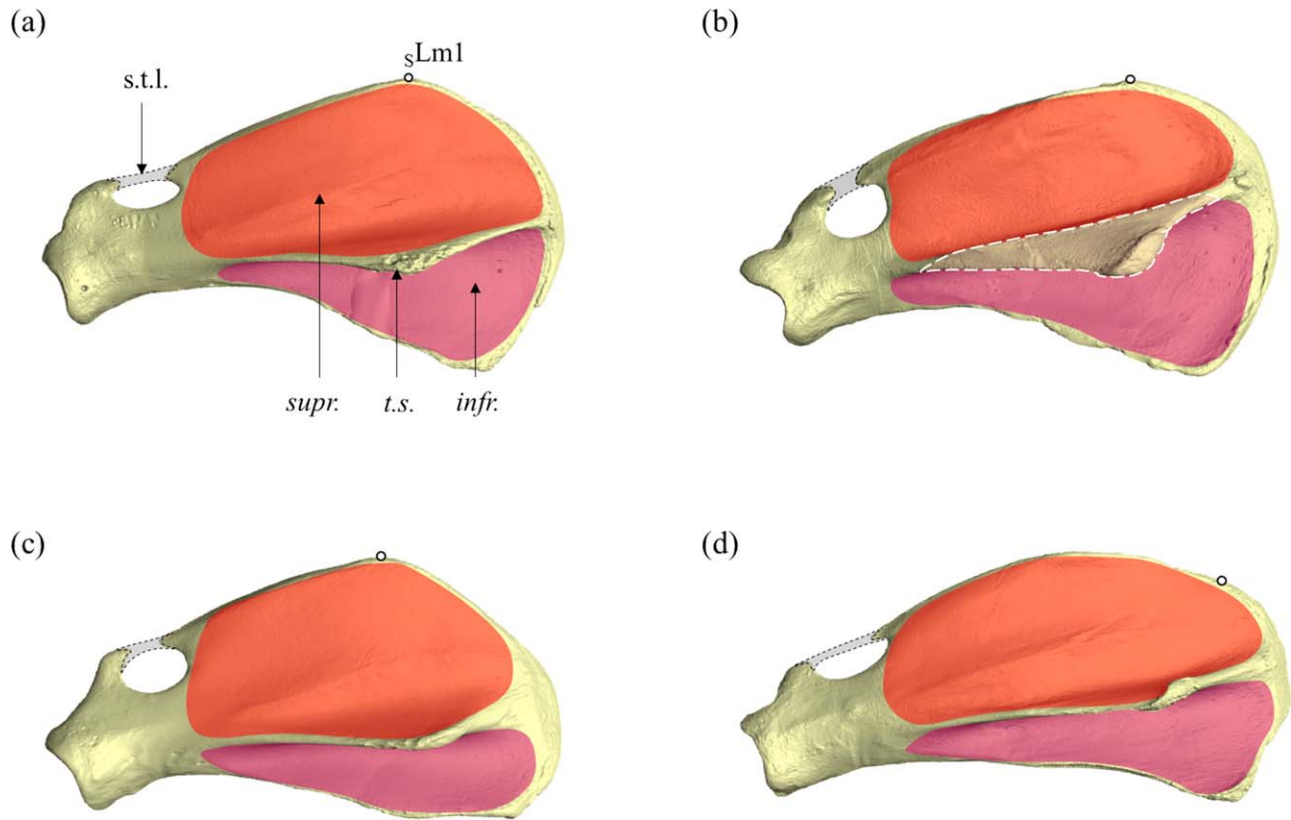


Fig. 4. Comparison of scapular blade morphology in tapirs. (a) *Tapirus bairdii*; (b) *T. indicus*; (c) *T. pinchaque*; (d) *T. terrestris*. Lateral view. Scapular features: SLM 1; *supr.* = supraspinous fossa (red); *infr.* = infraspinous fossa (purple); *t.s.* = tuber of the scapular spine; *s.t.l.*; superior transverse ligament.

tapir (*T. pinchaque*) is of particular note, with numerous morphological features in this species indicative of increased stride frequency and potentially higher locomotor speeds. Our study corroborates previous qualitative research on Malayan tapir (*T. indicus*) morphology, confirming a number of adaptations for increased weight-bearing in this species. We also identify similarities in the stylopodium and zeugopodium of the lowland (*T. terrestris*) and Baird's tapirs (*T. bairdii*), which may be correlated more closely with loading patterns (due to similar range of body mass) and habitat preferences rather than common ancestry.

Morphological Separation of the Mountain Tapir

Our results show that the upper forelimb bones of the mountain tapir (*T. pinchaque*) are consistently distinct from those of other extant tapirs. When inspecting landmark placement in the scapula of *T. pinchaque*, the cranial angle ($sLm\ 1$) midway along the cranial margin and the posteroventral placement of the scapular spine tuberosity ($sLm\ 3$) increase the area of the supraspinous fossa (Fig. 4). The scapular spine of *T. pinchaque* is more posteroventral than in any other

modern tapir, and the supraspinous fossa subsequently becomes much greater in relative area compared to the infraspinous (Fig. 4). Functionally, the supraspinous fossa is the attachment site for the *m. supraspinatus* and *m. subclavius*, which stabilize the scapula (Budras et al., 1999; Watson and Wilson, 2012). The infraspinous fossa is the principal attachment site for the *m. infraspinatus*, which primarily flexes the shoulder joint (Budras et al., 1999; Liebich et al., 2011) but has an additional role as a stabilizer. In other quadrupedal species, an enlarged *m. supraspinatus* has been suggested to allow for greater energy absorption on ground impact during locomotion (equids, Watson and Wilson, 2012; didelphid marsupials, Astúa, 2009). Despite recent research highlighting that the relationship between muscle attachment site and muscle volume is not necessarily a direct one (Bello-Hellegouarch et al., 2013; Larson and Stern, 1956), the *m. supraspinatus* in published studies of both *T. indicus* and *T. terrestris* fills or exceeds the supraspinous fossa (Murie, 2008; Windle and Parsons, 1901; Campbell, 2007; Bressou, 1936). Using this information, we interpret that a relatively large *m. supraspinatus* is present in *T. pinchaque*, facilitating greater stabilization

and shock absorption for the proximal limb (Watson and Wilson, 2012; Astúa, 2009). This has been shown to be useful for large taxa that use half-bounds during running locomotion (Astúa, 2009), a form of movement which is advantageous for rapid acceleration or deceleration (Walter and Carrier, 2012). The relatively enlarged *m. supraspinatus* may, therefore, enable *T. pinchaque* to use rapid deceleration when travelling through dense undergrowth on inclined surfaces without the innovation of more complex shock absorbers, such as those present in equids (Back et al., 1995).

The ratio of the scapular fossae areas (here described as the scapular fossa ratio; SFR) quantifies differences in supraspinous and infraspinous fossa size, confirming that *T. pinchaque* exhibits a larger supraspinous compared to infraspinous fossa than any other tapir in this study (Fig. 3). Although *T. pinchaque* displays the highest SFR of extant tapirs, all the neotropical tapirs exhibit higher SFRs than *T. indicus* and other extant perissodactyls (equids and rhinocerotids; Fig. 3). The supraspinous fossa morphology of *T. pinchaque* does not greatly resemble that of any modern ungulates (Maynard Smith and Savage, 2004), bearing more resemblance to the scapulae of felids (Zhang et al., 2012; Martín-Serra et al., 2010) and some basal perissodactyls (Kitts, 2007; Hellmund, 1985; Wood et al., 2010).

In addition to possessing a SFR higher than other tapir species, *T. pinchaque* exhibits the shallowest glenoid cavity of all the tapirs in this study (defined by sLm 9). A shallow glenoid cavity has been suggested to facilitate a high degree of mobility (Spoor and Badoux, 2006; Argot, 2013), rather than restricting the shoulder to a purely rotational movement. The higher degree of mobility in the shoulder joint may also help generate greater stride lengths in *T. pinchaque* by allowing more parasagittal movement of the humeral head within the shoulder joint. The combination of large supraspinous fossae and shallow glenoid cavities may act as a shock absorber in the proximal forelimb of *T. pinchaque*, in addition to a distal footpad. When compared to the impact resistance adaptations of other modern perissodactyls such as horses (Wilson et al., 2001), the modifications to the forelimb skeleton of *T. pinchaque* are less complex. In equids, the long tendons of the digital flexor muscles of the zeugopodium have evolved to act as impact dampeners (Wilson et al., 2001), associated with the loss of a foot pad (Thomason, 2005; MacFadden, 1993). This represents a derived, distal impact dampening adaptation. The osteological adaptations in *T. pinchaque* may have evolved to facilitate stable locomotion on the spongy “paramo” grassland, while also resisting impact forces when moving down inclined, alpine habitats (Downer, 2011; Downer, 1893; Watson and Wilson, 2012; Hawkins, 1954; Padilla et al., 1996), rather

than providing impact resistance for sustained running in open habitats (equids; MacFadden, 1993). Morphological adaptations in the scapular blade in *T. pinchaque*, in addition to overall scapular variability between extant tapir species (Figs. 3 and 4), offer evidence supporting the integral role the scapula plays in the kinematics of locomotion in quadrupeds, affecting stride length (Spoor and Badoux, 2006; Gasc, 1929; Schmidt and Fischer, 2006), stability (Spoor and Badoux, 2006; Argot, 2013; Wood et al., 2010), and impact cushioning (Watson and Wilson, 2012; Astúa, 2009; this study). However, it also highlights the capacity for large mammals within a single genus to display notable variation in their locomotor capabilities.

In addition to an unusual scapula shape, the humeri of *T. pinchaque* are more mediolaterally and craniocaudally narrow than those of other tapir species, giving the upper forelimb a more gracile appearance. The gracile nature of the upper forelimb elements in this study compliments similar observations of lower hind limb elements in *T. pinchaque* (Hawkins, 1954). The mediolateral narrowing of the limb bones reduces bone mass, creating less inertia for muscular action to overcome (Fedak et al., 2007; Carrano, 2008); this has been described as a “cursorial” adaptation, enabling an increased stride frequency (Gambaryan, 2012; Hildebrand, 2009; Van Valkenburgh, 2010; MacFadden, 1993; Carrano, 2008; Anton et al., 2005; Samuels et al., 2007).

The insertion sites of humeral flexors (e.g., teres tuberosity of the humerus) are more proximal to the joint centre than in any other tapir (H Lm 18; Fig. 5). In addition, the posteroventral positioning of the scapular spine alters the origination site for another shoulder flexor, the scapular head of the *m. deltoideus*. The proximal placement of muscle insertions (coupled with the posteroventral scapular spine) shortens the flexion lever arm around the shoulder joint for both the *m. teres major* and *m. deltoideus*, allowing less torque around the joint while enabling rapid flexion of the shoulder and adduction of the humerus (Gambaryan, 2012; Hildebrand, 2009; de Muizon and Argot, 2014; Pereira, 2013). This is another adaptation indicative of increased cursoriality (Gregory, 2005; Gambaryan, 2012; Hildebrand, 2009), and suggests that *T. pinchaque* may be capable of increased stride frequency compared to other extant tapirs.

In the zeugopodium (radius and ulna), *T. pinchaque* displays the least prominent lateral tuberosity of the radius (R Lms 4, 11), the site of attachment of the lateral collateral ligament. This tuberosity is described as prominent in most tapirs (Holbrook, 2013), cervids and sheep (Blagojević and Aleksić, 2012). The tuberosity is even more prominent in equids, rhinoceroses, and large bovines, projecting further than the lateral margin

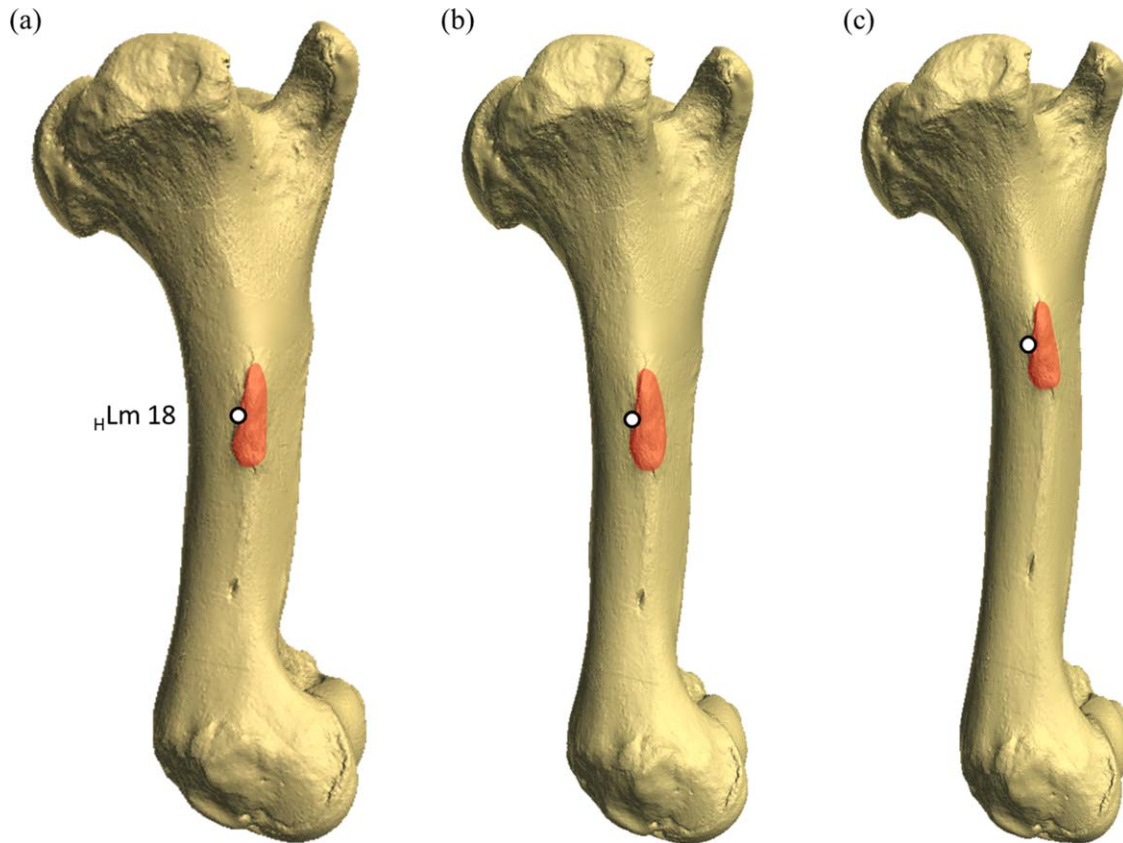


Fig. 5. Comparison between teres tuberosity positioning in *Tapirus*. From left: (a) *T. indicus*, (b) *T. terrestris*, and (c) *T. pinchaque*. All bones scaled to same size to make differences relative. Bone shapes based on mean average shape of species mapped onto surface scans of ZMB MAM 12999).

of the radial head (Gregory, 2005; Liebich et al., 2011). The lateral collateral ligament attachment of *T. pinchaque* is consistently found beneath the lateral extent of the radial head, a morphology more reminiscent of basal perissodactyls (Gregory, 2005; Radinsky, 1945; Holbrook, 2013; Wood et al., 2010), canids, and felids (Liebich et al., 2011; Argot, 2013). The functional interpretation of the lateral tuberosity placement beneath the radial head in *T. pinchaque* remains uncertain.

Finally, *T. pinchaque* exhibits the least amount of posterior rotation in the olecranon process of the ulna (Fig. 6). Caudal deflection of the olecranon (i.e., the angle of the olecranon to the long axis of the ulna) has been hypothesized to increase with overall body mass (Van Valkenburgh, 2010; de Muijon and Argot, 2014), and is described as an adaptation to weight-bearing in large ungulates (Gregory, 2005). *Tapirus pinchaque* exhibits the lowest angle of the olecranon (\perp Lm 15) to the long axis of the ulna (48.2°), compared to *T. terrestris* (62.8°) and *T. indicus* (66.5° ; Fig. 6). The angle at which the olecranon is offset from the long axis of the ulna determines the forelimb position in which the *m. triceps brachii* (zeugopodium extensor) has

the greatest leverage. In the case of *T. pinchaque*, the lower angle of deflection may imply a marginally more flexed forelimb position for maximum triceps leverage compared to other tapir species. Similar variations in olecranon morphology and caudal deflection have been observed in large felids (Christiansen and Adolfssen, 2015). These species possess similar overall body masses and implement their forelimbs in prey capture, thus care should be taken when comparing variation in osteological features in carnivores to similar variation observed in herbivores. However, tapirs in this study show a far greater range of body masses than those exhibited by large felids (Christiansen and Adolfssen, 2015), and we, therefore, interpret the more acute degree of olecranon rotation in *T. pinchaque* as indicative of lower loading on the forelimb in this species. In combination with the mediolaterally narrow humerus, radius and ulna, muscular and ligamentous attachment sites in the upper forelimb of *T. pinchaque* imply this species may be capable of higher stride frequency and potentially higher locomotor speeds than other modern tapirs.

The upper forelimb bones of *T. pinchaque* show a marked morphological contrast with its closest

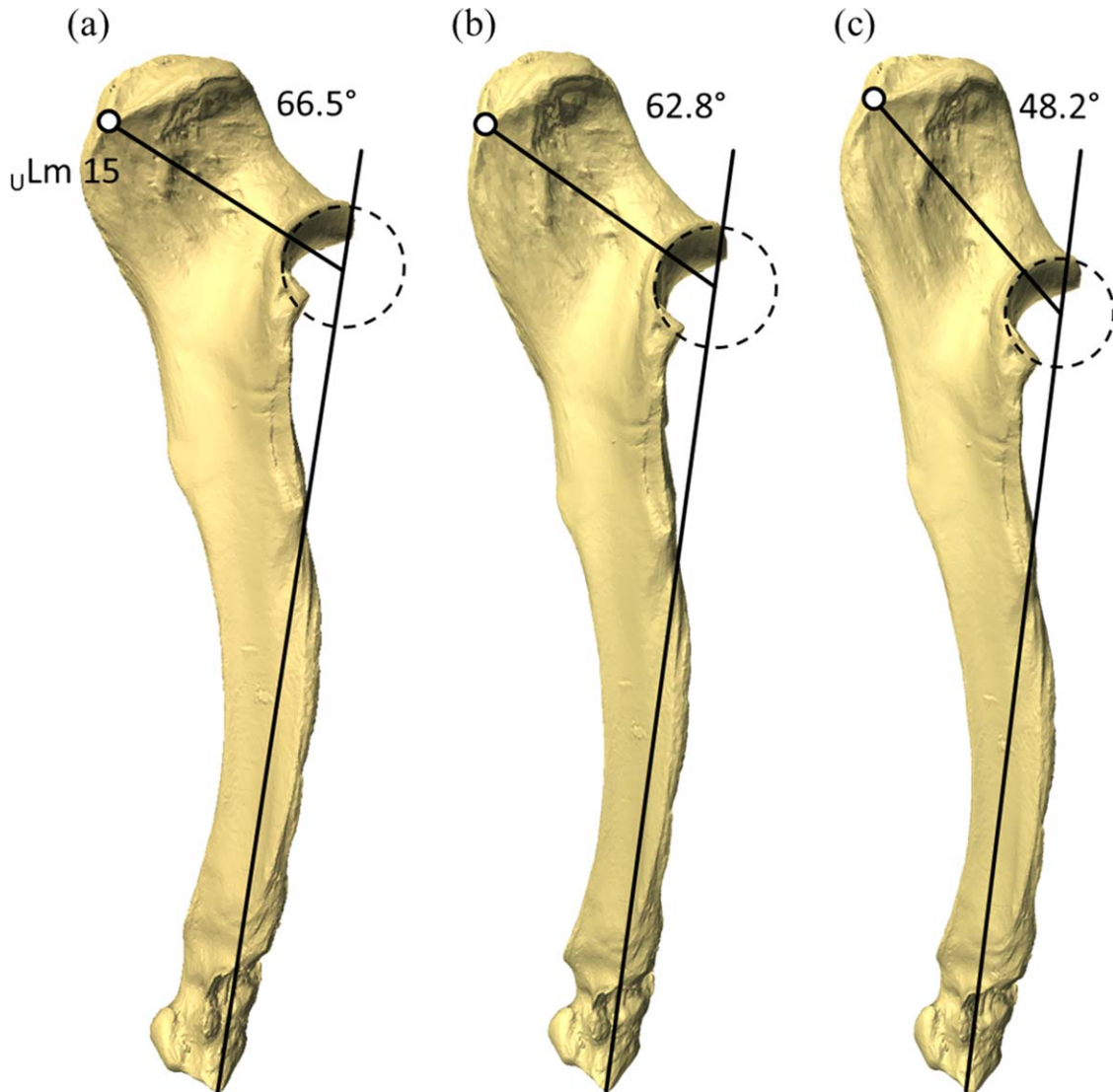


Fig. 6. Comparison between olecranon positioning in *Tapirus*. From left: (a) *T. indicus*, (b) *T. terrestris*, and (c) *T. pinchaque*. Angles between long axis of the ulna and ULm 15 decrease left to right. All bones scaled to same size to make differences relative. Bone shapes based on mean average shape of species mapped onto surface scans of RMNH 43495.

phylogenetic relative: *T. terrestris* (Figs. 2–6). Phylogenetic divergence estimates from molecular studies suggest these species began divergence recently in geological time (2–4 Mya; Steiner and Ryder, 2001; Ruiz-García et al., 1987, 1985; Cozzuol et al., 2012), with genetic differentiation between these species in some genes as low as 1% (Ruiz-García et al., 1985). There are significant differences between *T. pinchaque* and *T. terrestris* forelimb bone shapes, despite few differences in overall bone length (Supporting Information Tables 1, 2). As such, we conclude that the suite of morphological differences between *T. pinchaque* and other extant tapirs result from functional adaptations to a different locomotor style, most likely triggered by differences in habitat

exploitation (Lizcano et al., 1871; Padilla et al., 1996; Ruiz-García et al., 1987).

Adaptations to Weight-Bearing in the Malayan Tapir

Tapirus indicus is the only remaining Old World tapir (Holanda and Ferrero, 2010; de Thoisy et al., 2001), and has been shown to be morphologically, morphometrically, and molecularly separate from the neotropical taxa (Ferrero and Noriega, 1974; Holanda and Ferrero, 2010; Ruiz-García et al., 1987; Cozzuol et al., 2012; Ferrero, 2009). Our results corroborate findings from previous qualitative comparisons of forelimb osteology between *T. indicus* and *T. terrestris* (Earle, 2013; Gregory,

2005). Features of the upper forelimb which discriminate *T. indicus* correspond with results from previous studies claiming *T. indicus* is the most “graviportal” extant tapir (capable of powerful but slow locomotion; Gregory, 2005). Tapirs do not possess a passive stay apparatus of the forelimb (Hermanson and MacFadden, 2012), and must use upper forelimb muscles to maintain gravitational support.

The scapular spine (sLm 3) of *T. indicus* is more central on the blade than in other tapirs. Scapular spine placement reduces the supraspinous fossa area compared to the infraspinous, so reducing the SFR. The SFR of *T. indicus* is similar to that of modern rhinocerotids (Fig. 3), all of which exhibit numerous adaptations to weight-bearing (Gregory, 2005). A ventral deflection of the scapular spine, present in all our *T. indicus* specimens (visible in Fig. 4b), is described as indicative of species with high body masses (Gregory, 2005; Maynard Smith and Savage, 2004), and is interpreted as a further adaptation to greater body mass in *T. indicus* compared to other tapirs. This ventral deflection of the scapular spine was also present in the juvenile specimen of *T. indicus*, suggesting that this is a species-specific morphology and not necessarily correlated to increased body mass. This morphology is also present in smaller modern ungulates (< 200 kg) such as pygmy hogs (*Porcula salvania*) and domestic suids (Oliver, 1966; Liebich et al., 2011; Deka et al., 1995), suggesting an additional functional role.

The lesser and greater tubercles of the humerus (H Lms 2, 4, 7) are expanded both proximally and laterally of the shoulder articulation. Tubercle morphology discriminates *T. indicus* humeri from those of other modern tapirs. The tubercles provide large insertion sites and confer greater mechanical advantage to the muscles that stabilize the shoulder joint (Hermanson and MacFadden, 2012). In a similar fashion, the craniocaudally thickened olecranon offers a greater insertion site for the heads of the *m. triceps brachii*, suggesting a larger elbow extensor. Greater leverage is accomplished during elbow extension by the angle of caudal deflection of the olecranon in *T. indicus* (Van Valkenburgh, 2010), higher than is present in other species (Fig. 6). From this morphology, we infer that the forelimb of *T. indicus* experiences greater loading than other extant tapirs during both locomotion and stationary stance. Adaptations to the shoulder and elbow joints observed in *T. indicus*, such as the large infraspinous fossa, expanded humeral tubercles, and large caudal angle of the olecranon are typical of “graviportal” ungulates (Gregory, 2005; Maynard Smith and Savage, 2004; Hermanson and MacFadden, 2012). Thus, the osteological features of the upper forelimb which contributed toward successful discrimination between *T. indicus* and other tapirs

highlighted adaptations for maintaining gravitational support and successful locomotion with higher body mass in *T. indicus*.

Morphological Position of the Lowland and Baird's Tapirs

Our landmark-based shape differences did not always result in successful discrimination, especially between species with similar overall body mass ranges (de Thoisy et al., 2001). The neotropical lowland tapir (*T. terrestris*) and Baird's tapir (*T. bairdii*) overlap in their range of body masses (*T. terrestris*: 160–295 kg; *T. bairdii*: 180–340 kg; de Thoisy et al., 2001), and in several of their forelimb bone shapes (this study). The scapular shape of *T. bairdii* is significantly dissimilar to that of *T. terrestris*; however, the long bone shape of *T. bairdii* and *T. terrestris* are shown to be the most similar of any extant tapir species. On several occasions *T. terrestris* and *T. bairdii* bones were so similar that the discriminant analysis could not separate these species. Similarities may be due to comparable loading on the limb during locomotion, influenced by a similar range of body masses in these species (de Thoisy et al., 2001). In addition, similarities in morphology may have arisen through common ancestry or similar habitat preferences. The lineages leading to these two species diverged from one another 9–11 Mya (Colbert, 2013; Ruiz-García et al., 1987), and thus represent two separate lineages of neotropical tapirs (Hulbert, 2009; García et al., 2014; Ruiz-García et al., 1987). The lineage of *T. bairdii* has been suggested to have secondarily migrated into Central America after the colonization of South America by the ancestor of *T. terrestris* and *T. pinchaque* during the Great American Biotic Interchange (García et al., 2014; Cione et al., 2005). *T. bairdii* shows greater phylogenetic affinity to the now extinct North American tapir subgenus *Helicotapirus* (Ferrero and Noriega, 1974; Hulbert, 2009; Holanda and Ferrero, 2010), which may have originated from a South American ancestor (Hulbert, 2009; Holanda and Ferrero, 2010). Phylogenetically, *T. terrestris* is most closely related to *T. pinchaque*, having diverged approximately 2–4 Mya (Steiner and Ryder, 2001; Ruiz-García et al., 1987, 1985). These two sister taxa exhibit extensive morphological differences, despite sharing a more recent common ancestor than *T. bairdii* and *T. terrestris* (Steiner and Ryder, 2001; Ruiz-García et al., 1987, 1985; Cozzuol et al., 2012). The similarity between the long bones of *T. terrestris* and *T. bairdii* may be explained by other biotic and abiotic factors (e.g., body mass, habitat), although common ancestry cannot be entirely ruled out as an influencing factor. Populations of *T. bairdii* and *T. terrestris* are known to occur in similar habitats in their respective geographical ranges, with some

sympatric populations in upland forest regions of Colombia (Padilla et al., 1996; González-Maya et al., 2011; Ruiz-García et al., 1987). We, therefore, conclude that these two species exhibit similarities in their stylopodium and zeugopodium due to both phylogenetic (common ancestry) and behavioral (comparable habitat use and overall range of body masses) influences. In addition, an increased sample size may reveal more subtle variations between these misclassified groups. Small sample sizes in highly disparate a priori groups are not as problematic as for morphologically similar groups. As such, increasing the sample size for groups that are more frequently misclassified may increase the power of the analyses, and increase accurate classification (Lachenbruch, 2014; Brennan et al., 2003; Davis and McHorse, 2003). This represents an intrinsic limitation for our study. However, factors affecting the dissimilarity in scapular shape between *T. terrestris* and *T. bairdii* are less easy to determine, and may be influenced by phylogenetic separation. Investigations into the forelimb osteology of extinct South American tapirs most closely related to *T. terrestris* (e.g., *T. cristatellus*, *T. rondoniensis*) may reveal whether phylogenetic relatedness is a factor influencing the divergence in scapular morphology between *T. terrestris* and *T. bairdii*.

CONCLUSIONS

Modern tapirs exhibit interspecific differences in the bone morphologies in their upper forelimb skeleton. The scapula exhibits the greatest degree of interspecific variation and is revealed as the most diagnostic bone in the upper forelimb (using DFA of three-dimensional landmark data). Our study corroborates all previous analyses comparing the Malayan (*T. indicus*) and lowland (*T. terrestris*) tapirs: *T. indicus* not only possesses the largest bones of the extant tapirs, but also exhibits a suite of osteological features associated with increased limb loading. Key morphological differences between tapirs revealed in this study centre around the mountain tapir (*T. pinchaque*). The morphological features of the scapula that discriminate *T. pinchaque* (large supraspinous fossa, posteroventrally positioned scapular spine) are unique within modern ungulates. This species also possesses long humeri, radii, and ulnae relative to its more massive neotropical relatives (e.g., *T. terrestris* and *T. bairdii*). All these adaptations hint at subtly different locomotion styles in extant tapirs. Acquisition of comparative data on autopodial bones (carpals, metacarpals, and phalanges) will be the next step in further understanding differences in locomotor morphology between modern tapirs.

ACKNOWLEDGMENTS

The authors would like to thank Chris Conroy (MVZ), Christiane Funk (ZMB), Eleanor Hoeger (AMNH), Pepijn Kamminga (RMNH), Josephine Lesur (MNHN), Luc Tyteca (MEO), and Frank Zachos (NHMW) for provision of museum specimens for this study. JM would like to thank Nele Tomsin and Hester Hanegraef for scanning assistance, Francis Vercaammen (KMDA) for providing dissection specimen, and Brianna McHorse, Denise Vogel, and Chris Van Ginneken for their help during dissection. The authors would also like to thank two anonymous reviewers for their helpful comments and remarks during the revision process. Author Contributions: All authors conceived and developed the study. JM collected the data and performed the analyses. JM and SN interpreted the data. JM wrote the manuscript, with significant contributions from SN. JM designed and prepared the figures.

LITERATURE CITED

- Alrtib AM, Philip CJ, Abdunnabi AH, Davies HM. 2013. Morphometrical study of bony elements of the forelimb fetlock joints in horses. *Anat Histol Embryol* 42:9–20.
- Andersson K. 2004. Elbow-joint morphology as a guide to forearm function and foraging behaviour in mammalian carnivores. *Zool J Linn Soc* 142:91–104.
- Andersson K, Werdelin L. 2003. The evolution of cursorial carnivores in the Tertiary: implications of elbow-joint morphology. *Proc R Soc B: Biol Sci* 270(Suppl. 2): S163–S165.
- Anton M, Galobart A, Turner A. 2005. Co-existence of scimitar-toothed cats, lions and hominins in the European Pleistocene. Implications of the post-cranial anatomy of (Owen) for comparative palaeoecology. *Quat Sci Rev* 24:1287–1301.
- Argot C. 2013. Postcranial analysis of a carnivoran-like archaic ungulate: the case of *Arctocyon primaevus* (Arctocyonidae, Mammalia) from the Late Paleocene of France. *J Mamm Evol* 20:83–114.
- Astúa D. 2009. Evolution of scapula size and shape in didelphid marsupials (Didelphimorphia: Didelphidae). *Evolution* 63: 2438–2456.
- Back W, et al. 1995. How the horse moves: 1. Significance of graphical representations of equine forelimb kinematics. *Equine Vet J* 27:31–38.
- Bassarova M, Janis CM, Archer M. 2008. The calcaneum—on the heels of marsupial locomotion. *J Mamm Evol* 16:1–23.
- Bello-Hellegouarch G, et al. 2013. A comparison of qualitative and quantitative methodological approaches to characterizing the dorsal side of the scapula in Hominoidea and its relationship to locomotion. *Int J Primatol* 34:315–336.
- Bernor RL, Scott RS, Haile-Selassie Y. 2005. A contribution to the evolutionary history of Ethiopian hipparionine horses (Mammalia, Equidae): Morphometric evidence from the post-cranial skeleton. *Geodiversitas* 27:133–158.
- Bignon O, et al. 2005. Geometric morphometrics and the population diversity of late glacial horses in Western Europe (*Equus caballus arcelini*): Phylogeographic and anthropological implications. *J Archaeol Sci* 32:375–391.
- Blagojević M, Aleksić J. 2012. Forensic analysis of bone in *Regio antibrachii* of deer (*Capreolus capreolus*) and sheep (*Ovis aries*) in order to determine origin of animal species. *Vet Glasnik* 66:325–331.
- Budras K-D, Sack WO, Rock S. 2003. Thoracic limb. In K-D. Budras, W.O. Sack, S. Rock, editors. *Anatomy of the Horse*. Stuttgart: Schlutersche, pp 2–13.

- Campbell B. 1936. The comparative myology of the forelimb of the hippopotamus, pig and tapir. *Am J Anat* 59:201–247.
- Carrano MT. 1999. What, if anything, is a cursor? Categories versus continua for determining locomotor habit in mammals and dinosaurs. *J Zool* 247:29–42.
- Christiansen P, Adolfssen JS. 2007. Osteology and ecology of *Megantereon cultridens* SE311 (Mammalia; Felidae; Machairodontinae), a sabrecat from the Late Pliocene - Early Pleistocene of Senéze, France. *Zool J Linn Soc* 151:833–884.
- Cignoni P, Callieri M, Corsini M, Dellapiane M, Ganovelli F, Ranzuglia G. 2008. MeshLab: an open-source mesh processing tool. In Scarano V, De Chiara R, Erra U, editors. *Eurographics Italian Chapter Conference*. Salerno, pp. 1–8.
- Cione AL, Gasparini GM, Soibelzon E, Leopoldo HS, Eduardo PT. 2015. The great American biotic interchange: A South American perspective. In: Cione AL, Gasparini GM, Soibelzon E, Leopoldo HS, Eduardo PT, editors. *New York: Springer*.
- Clayton HM, Chateau H, Back W. 2013. Forelimb function. In: Back W, Clayton HM, editors. *Equine Locomotion*. London: Saunders Elsevier, pp 99–125.
- Colbert M. 2005. The facial skeleton of the early Oligocene *Colodon* (Perissodactyla, Tapiroidea). *Palaeontol Electron* 8: 1–27.
- Constantinescu GM, Habel RE, Hillebrand A, Sack WO, Schaller O, Simoens P, de Vos NR. 2012. Illustrated Veterinary Anatomical Nomenclature Third. In: Constantinescu GM, Schaller O, editors. *Stuttgart: Enke*.
- Cozzuol MA, Clozato CL, Holanda EC, Rodrigues FHG, Nienow S, de Thoisy B, Redondo RAF, Santos FR. 2013. A new species of tapir from the Amazon. *J Mammal* 94:1331–1345.
- Cozzuol MA, de Thoisy B, Fernandes-Ferreira H, Rodrigues FHG, Santos FR. 2014. How much evidence is enough evidence for a new species? *J Mammal* 95:899–905.
- Curran SC. 2012. Expanding ecomorphological methods: geometric morphometric analysis of Cervidae post-crania. *J Archaeol Sci* 39:1172–1182.
- Curran SC. 2015. Exploring Eucladoceros ecomorphology using geometric morphometrics. *Anat Rec* 298:291–313.
- Deka A, Baishya G, Das BJ, Talukdar M, Kalita PC. 2013. Gross anatomy of the scapula of pygmy hog (*Porcula salvania*). *Indian J Vet Anat* 25:109–110.
- de Muizon C, Argot C. 2003. Comparative anatomy of the Tiupampa didelphimorphs; an approach to locomotory habits of early marsupials. In: Jones M, Dickman C, Archer M, editors. *Predators with Pouches: The Biology of Carnivorous Marsupials*. Collingwood: Csiro, pp 43–62.
- de Thoisy B, Pukazhenti B, Janssen, D.L., Torres, I.L., May Jr., J.A., Medici, P., Mangini, P.R., Marquez, P. A.B., Vanstreels, R.E. T., Fernandes-Santos, R.C., Hernandez-Divers, S. & Quse, V., 2014. *Tapir Veterinary Manual* 2nd ed. V. Quse & R.C. Fernandes-Santos, eds., Campo Grande: IUCN/SSC Tapir Specialist Group, pp.1–155.
- Downer CC. 2001. Observations on the diet and habitat of the mountain tapir (*Tapirus pinchaque*). *J Zool* 254:279–291.
- Downer CC. 1995. The gentle botanist. *Wildlife Conserv* 98:30–35.
- Earle C. 1893. Some points in the comparative osteology of the tapir. *Science* 21:118.
- Elissamburu A, de Santis L. 2011. Forelimb proportions and fossorial adaptations in the scratch-digging rodent *Ctenomys* (Caviomorpha). *J Mammal* 92:683–689.
- Evans HE, de Lahunta A. 2013. Appendicular Skeleton. In Evans HE, de Lahunta A, editors. *Miller's Anatomy of the Dog*. St. Louis: Elsevier, pp 127–151.
- Fabre A-C, et al. 2014. A three-dimensional morphometric analysis of the locomotory ecology of *Deccanolestes*, a eutherian mammal from the Late Cretaceous of India. *J Vertebrate Paleontol* 34:146–156.
- Fabre A-C, Cornette R, et al. 2015. Do constraints associated with the locomotor habitat drive the evolution of forelimb shape? A case study in musteloid carnivorans. *J Anat* 226: 596–610.
- Fabre A-C, et al. 2013. Getting a grip on the evolution of grasping in musteloid carnivorans: A three-dimensional analysis of forelimb shape. *J Evol Biol* 26:1521–1535.
- Fabre A-C, Salesa MJ, et al. 2015. Quantitative inferences on the locomotor behaviour of extinct species applied to *Simocyon batalleri* (Ailuridae, Late Miocene, Spain). *Die Naturwissenschaften* 102:1280.
- Fedak M, Heglund N, Taylor C. 1982. Energetics and mechanics of terrestrial locomotion. II. Kinetic energy changes of the limbs and body as a function of speed and body size in birds and mammals. *J Exp Biol* 97:23–40.
- Ferrero B. 2013. A taxonomic and biogeographic review of the fossil tapirs from Bolivia. *Acta Palaeontol Pol* 59:505–516.
- Ferrero BS, Noriega JI. 2007. A new upper Pleistocene tapir from Argentina: Remarks on the phylogenetics and diversification of neotropical Tapiridae. *J Vertebrate Paleontol* 27: 504–511.
- Flores DA, Díaz MM. 2009. Postcranial skeleton of *Glironia venusta* (Didelphimorphia, Didelphidae, Caluromyinae): Description and functional morphology. *Zoosyst Evol* 85:311–339.
- Gambaryan PP. 1974. *How Mammals Run: Anatomical Adaptations*. New York: Wiley.
- García MJ, et al. 2012. Distribution, habitat and adaptability of the genus *Tapirus*. *Integr Zool* 7:346–355.
- González-Maya JF, et al. 2012. Baird's tapir density in high elevation forests of the Talamanca region of Costa Rica. *Integr Zool* 7:381–388.
- Gould FDH. 2014. To 3D or not to 3D, that is the question: Do 3D surface analyses improve the ecomorphological power of the distal femur in placental mammals? *PLoS One* 9:e91719.
- Gregory WK. 1929. *Mechanics of locomotion in the evolution of limb structure as bearing on the form and habits of the titanotheres and the related odd-toed ungulates*. In: Osborn HF, editor. *The Titanotheres of Ancient Wyoming, Dakota and Nebraska*. Washington, DC: United States Government Printing Office, pp 727–756.
- Halenar LB. 2011. Reconstructing the locomotor repertoire of *Protopithecus brasiliensis*. II. Forelimb morphology. *Anat Rec* 294:2048–2063.
- Hawkins PL. 2011. Variation in the Modified First Metatarsal of a Large Sample of *Tapirus polkensis*, and the Functional Implication for Ceratomorphs. Johnson City: East Tennessee State University, pp 1–99.
- Hellmund M. 2005. A three-dimensional skeletal reconstruction of the Middle Eocene *Propalaeotherium hassiacum* Haupt 1925 (Equidae, Perissodactyla, Mammalia) and a. In *Current Research in Vertebrate Palaeontology 3rd Annual Meeting of the European Association of Vertebrate Palaeontologists (EAVP)*. Hessisches Landesmuseum Darmstadt, Darmstadt. p 15.
- Hermanson JW, MacFadden BJ. 1992. Evolutionary and functional morphology of the shoulder region and stay-apparatus in fossil and extant horses (Equidae). *J Vertebrate Paleontol* 12:377–386.
- Hershkovitz P. 1954. *Mammals of Northern Colombia, Preliminary Report No. 7: Tapirs (genus Tapirus) with a Systematic Review of American species*. *Proc US Natl Mus* 103:465–496.
- Hildebrand M. 1985. *Walking and running*. In: Hildebrand M, Bramble DM, Liem KF, Wake DB, editors. *Functional Vertebrate Morphology*. Cambridge: Harvard University Press, pp 38–57.
- Holanda EC, Ferrero BS. 2012. Reappraisal of the genus *Tapirus* (Perissodactyla, Tapiridae): Systematics and phylogenetic affinities of the South American tapirs. *J Mamm Evol* 20:33–44.
- Holbrook L. 2001. Comparative osteology of early Tertiary tapiromorphs (Mammalia, Perissodactyla). *Zool J Linn Soc* 132:1–54.
- Holbrook LT. 2009. Osteology of *Lophiodon* Cuvier, 1822 (Mammalia, Perissodactyla) and its phylogenetic implications. *J Vertebrate Paleontol* 29:212–230.

- Hulbert RC. 2010. A new early Pleistocene tapir (Mammalia: Perissodactyla) from Florida, with a review of Blancan tapirs from the state. *Bull Florida Mus Nat Hist* 49:67–126.
- IBM Corp. 2013. IBM SPSS Statistics for Windows, Version 22.0. Armonk, NY: IBM Corp.
- Janis C. 1984. Tapirs as Living Fossils. In: Eldredge N, Stanley SM, editors. *Living Fossils. Casebooks in Earth Sciences*. New York, NY: Springer New York. pp 80–86.
- Jenkins FA Jr. 1973. The functional anatomy and evolution of the mammalian humero-ulnar articulation. *Am J Anat* 137: 281–297.
- Kaushik N. 2009. A quantitative analysis of European horses from Pleistocene to Holocene. Vila Real: Universidade de Trás-os-Montes e Alto Douro. pp 1–73.
- Kitts DB. 1956. American *Hyracotherium* (Perissodactyla, Equidae). *Bull Am Mus Nat Hist* 110:1–60.
- Klingenberg CP. 2011. MorphoJ: An Integrated Software Package for Geometric Morphometrics. *Mol Ecol Resour* 11:353–357.
- Kuncova P, Frynta D. 2009. Interspecific morphometric variation in the postcranial skeleton in the genus *Apodemus*. *Belg J Zool* 139:133–146.
- Larson SG, Stern JT. 2013. Rotator cuff muscle function and its relation to scapular morphology in apes. *J Hum Evol* 65:391–403.
- Liebich H-G, König HE, Maierl J. 2007. Forelimb or thoracic limb (membra thoracica). In: König HE, Liebich H-G, editors. *Veterinary Anatomy of Domestic Animals: Textbook and Colour Atlas*. Stuttgart: Schlutersche, pp 145–214.
- MacFadden BJ. 1992. *Fossil Horses: Systematics, Paleobiology and Evolution of the Family Equidae*. Cambridge: Cambridge University Press.
- Martínez-Navarro B., Rabinovich R. 2011. The fossil Bovidae (Artiodactyla, Mammalia) from Gesher Benot Ya'aqov, Israel: Out of Africa during the Early-Middle Pleistocene transition. *J Hum Evol* 60:375–386.
- Martín-Serra A, Figueirido B, Palmqvist P. 2014. A three-dimensional analysis of morphological evolution and locomotor performance of the carnivoran forelimb. *PLoS One* 9:e85574.
- Maynard Smith J, Savage RJG. 1956. Some locomotory adaptations in mammals. *J Linn Soc Lond Zool* 42:603–622.
- Meloro C. 2011. Locomotor adaptations in Plio-Pleistocene large carnivores from the Italian peninsula: palaeoecological implications. *Curr Zool* 57:269–283.
- Murie J. 1871. The Malayan tapir. *J Anat Physiol* 6:131–512.
- Oliver WLR, editor. 1993. *Status Survey and Conservation Action Plan: Pigs, Peccaries and Hippos, Gland, Switzerland: IUCN/SSC Pigs and Peccary Specialist Group*.
- Padilla M, Dowler RC. 1994. *Tapirus terrestris*. *Mamm Species* 481:1–8.
- Padilla M, Dowler RC, Downer CC. 2010. *Tapirus pinchaque* (Perissodactyla: Tapiridae). *Mamm Species* 42:166–182.
- Payne RC, Veenman P, Wilson AM. 2004. The role of the extrinsic thoracic limb muscles in equine locomotion. *J Anat* 205: 479–490.
- Pereira SG. 2013. *Anatomia Ossea, Muscular e Considerações Adaptativas do Membro Torácico de Tapirus Terrestris* (Perissodactyla, Tapiridae). Santa Mônica: Universidade Federal de Uberlândia. pp 1–76.
- R Development Core Team. 2008. *R: A Language and Environment for Statistical Computing*. Vienna, Austria: R Foundation for Statistical Computing. ISBN 3-900051-07-0.
- Radinsky L. 1966. The adaptive radiation of the phenacodontid condylarths and the origin of the Perissodactyla. *Evolution* 20:408–417.
- Radinsky LB. 1965. Evolution of the tapiroid skeleton from *Heptodon* to *Tapirus*. *Bull Mus Comp Zool* 134:69–106.
- Rose KD. 1996. Skeleton of early Eocene *Homogalax* and the origin of Perissodactyla. *Palaeovertebrata* 25:243–260.
- Ruiz-García M, Vásquez C, Pinedo-Castro M, Sandoval S, Castellanos A, Kaston F, de Thoisy B, Shostell J. 2012. Phylogeography of the mountain tapir (*Tapirus pinchaque*) and the Central American tapir (*Tapirus bairdii*) and the origins of the three Latin-American tapirs by means of mtCyt-B sequences. In: Ananthawat-Jnsson K, editor. *Current Topics in Phylogenetics and Phylogeography of Terrestrial and Aquatic Systems*. Rijeka: InTech. pp 83–116.
- Samuels JX, Meachen JA, Sakai SA. 2013. Postcranial morphology and the locomotor habits of living and extinct carnivorans. *J Morphol* 274:121–146.
- Samuels JX, Van Valkenburgh B. 2008. Skeletal indicators of locomotor adaptations in living and extinct rodents. *J Morphol* 269:1387–1411.
- Simpson G. 1945. Notes on Pleistocene and recent tapirs. *Bull Am Mus Nat Hist* 86:33–82.
- Spoor CF, Badoux DM. 1986. Descriptive and functional myology of the neck and forelimb of the striped hyena (*Hyaena hyaena*, L. 1758). *Anatomischer Anzeiger* 161:375–387.
- Steiner CC, Ryder OA. 2011. Molecular phylogeny and evolution of the Perissodactyla. *Zool J Linn Soc* 163:1289–1303.
- Thomason JJ. 1985. Estimation of locomotory forces and stresses in the limb bones of recent and extinct equids. *Paleobiology* 11:209–220.
- Van Valkenburgh B. 1987. Skeletal indicators of locomotor behavior in living and extinct carnivores. *J Vertebrate Paleontol* 7:162–182.
- Walter RM, Carrier DR. 2007. Ground forces applied by galloping dogs. *J Exp Biol* 210:208–216.
- Watson JC, Wilson AM. 2007. Muscle architecture of biceps brachii, triceps brachii and supraspinatus in the horse. *J Anat* 210:32–40.
- Weisbecker V, Warton DI. 2006. Evidence at hand: diversity, functional implications, and locomotor prediction in intrinsic hand proportions of diprotodontian marsupials. *J Morphol* 267:1469–1485.
- Wiley DF. 2006. *Landmark Editor 3.0*. IDAV, Davis: University of California. Available at: <http://graphics.idav.ucdavis.edu/research/EvoMorph>
- Wilson AM, et al. 2001. Horses damp the spring in their step. *Nature* 414:895–899.
- Wilson DE, Reeder DM. 2005. *Mammal Species of the World: A Taxonomic and Geographical Reference* 3rd ed. In: Wilson DE, Reeder DM, editors. Baltimore: Johns Hopkins University Press. pp 142.
- Wood AR, et al. 2010. Postcranial functional morphology of *Hyracotherium* (Equidae, Perissodactyla) and locomotion in the earliest horses. *J Mamm Evol* 18:1–32.
- Zelditch ML, Swiderski DL, Sheets HD. 2012. *Geometric Morphometrics for Biologists: A Primer*. New York: Academic Press.
- Zhang KY, et al. 2012. 3D morphometric and posture study of felid scapulae using statistical shape modelling. *PLoS One* 7: e34619.